Topological Criticality in the Chiral-Symmetric AIII Class at Strong Disorder

Ian Mondragon-Shem and Taylor L. Hughes
Department of Physics, University of Illinois-Urbana Champaign, Urbana, Illinois 61801, USA

Juntao Song and Emil Prodan
Department of Physics, Yeshiva University, New York, New York 10016, USA

(Received 7 December 2013; published 23 July 2014)

The chiral AIII symmetry class in the classification table of topological insulators contains topological phases classified by a winding number ν for each odd space dimension. An open problem for this class is the characterization of the phases and phase boundaries in the presence of strong disorder. In this work, we derive a covariant real-space formula for ν and, using an explicit one-dimensional disordered topological model, we show that ν remains quantized and nonfluctuating when disorder is turned on, even though the bulk energy spectrum is completely localized. Furthermore, ν remains robust even after the insulating gap is filled with localized states, but when the disorder is increased even further, an abrupt change of ν to a trivial value is observed. Using exact analytic calculations, we show that this marks a critical point where the localization length diverges. As such, in the presence of disorder, the AIII class displays markedly different physics from everything known to date, with robust invariants being carried entirely by localized states and bulk extended states emerging from an absolutely localized spectrum. Detailed maps and a clear physical description of the phases and phase boundaries are presented based on numerical and exact analytic calculations.

DOI: 10.1103/PhysRevLett.113.046802 PACS numbers: 73.20.Fz, 73.21.Hb, 73.61.Ng

In the classification table of topological insulators and superconductors [1–3], the unitary class A is arguably the most well understood, especially in the presence of disorder. Here, in even space dimensions, the topological phases are characterized by the Chern invariants [4], which are robust against disorder and are carried by bulk extended states that are embedded within a large set of localized states [5–8]. When the disorder is increased, the bulk extended states above and below the Fermi level E_F levitate toward one another in the energy spectrum and then annihilate upon collision, leading to topological phase transitions where the localization length diverges. This complete picture that we have for class A, and which was also observed in several other symmetry classes [9–12], is often assumed to apply to all symmetry classes in the classification table.

The AIII chiral-unitary class in odd space dimensions is the natural partner of the A unitary class [1,13], and one would expect a close similarity in their behavior at strong disorder. In this Letter, we demonstrate similarities but also several striking differences between the two symmetry classes. First, we derive and compute a covariant, self-averaging, real-space formula for ν in any odd dimension. For a generic one-dimensional (1D) two-band model in the AIII class, ν is found to remain quantized and nonfluctuating even after the disorder completely fills the spectral gap with localized states. When increasing the disorder even further, a sharp drop of ν is observed from the topological to the trivial value. We derive an analytical formula for the localization length $\Lambda(E)$ of the model at energy $E = 0$ and show that it diverges at this transition point. The similarities with the A-symmetry class, however, end here. Using several established numerical methods, we find that the entire bulk energy spectrum is entirely localized immediately after the disorder is turned on. As the disorder is increased, the energy spectrum remains localized until the transition point is reached and a divergence of $\Lambda(E)$ strictly at $E = 0$ develops. These findings demonstrate that robust topological numbers can be carried entirely by localized states and that disorder can drive a completely localized topological phase through a delocalized critical point, in total contrast with the present status quo on disordered topological insulators.

To understand the physical mechanism of the topological phase transition, we map the disordered tight-binding model into a spin-1/2 Hamiltonian via a Jordan-Wigner transformation, which enables us to write the ground state as a product state constructed from the single-particle states with weights on only two sites for all Hamiltonian parameters and disorder strengths except exactly at the critical point. From here, we can show explicitly that the topological invariant is shared among all localized states and that the phase transition is driven by a proliferation of low-energy modes which ultimately lead to the divergence of the localization length and of the density of states at $E = 0$.

The disordered model we work with is

$$H = \sum_{n\in\mathbb{Z}} \left\{ t_n \left[\frac{1}{2} c_n^\dagger (\sigma_1 + i\sigma_2) c_{n+1} + \text{H.c.} \right] + m_n c_n^\dagger \sigma_2 c_n \right\}, \tag{1}$$

where σ_α's are Pauli's matrices and $c_n^\dagger = (c_{n,A}^\dagger, c_{n,B}^\dagger)$ creates particles of orbital type A or B at site n. The disorder is present on both the hopping and on-site potentials: $t_n = 1 + W_1\omega_n$ and $m_n = m + W_2\omega_n'$, where ω_n and ω_n' are independent randomly generated numbers drawn from the uniform distribution $[-0.5, 0.5]$. The model preserves only the chiral symmetry $SHS^{-1} = -H$, with $S = \sum_n c_n^\dagger \sigma_3 c_n$, as the last term in Eq. (1) breaks both the particle-hole ($= \sigma_3 K$) and time-reversal ($= K$, the complex conjugation) symmetries. Despite the model's simplicity, its behavior is representative for the 1D AIII class because any gapped chiral-symmetric system can be adiabatically deformed into an independent sum of two-band models like Eq. (1).

In the clean limit $W_{1,2} = 0$, the Bloch Hamiltonian takes the form

$$h(k) = \begin{pmatrix} 0 & e^{ik} - im \\ e^{-ik} + im & 0 \end{pmatrix}, \quad \sigma_3 h(k) \sigma_3^{-1} = -h(k). \tag{2}$$

The topological invariant of the model is given by the winding number of the off-diagonal block of $h(k)$ [14]:

$$\nu = \int_0^{2\pi} \frac{\partial_k (e^{ik} - im)}{e^{ik} - im} \frac{dk}{2\pi i} = \begin{cases} 1 \text{ if } m \in (-1, 1) \\ 0 \text{ otherwise.} \end{cases} \tag{3}$$

The bulk energy gap closes precisely at $m = \pm 1$, which signals the topological phase transitions in the clean system. In general, ν can take on any integer value, and if $n_\pm$ denote the numbers of bound states of each chirality at one end of an open chain, then topology enforces the bulk-edge correspondence: $\nu = \pm(n_+ - n_-)$. ν can also be expressed as a "skew polarization":

$$\nu = \frac{1}{\pi} \int_0^{2\pi} dk \tilde{A}(k), \quad \tilde{A}(k) = i \sum_{\alpha \in \text{occ}} \langle S u_\alpha(k) | \partial_k | u_\alpha(k) \rangle, \tag{4}$$

where $|u_\alpha(k)\rangle$ is the Bloch function for band α. Equation (4) enables us to establish (see the Supplemental Material [15]) the relation $2P = \nu \bmod 2$, where P is the standard electric polarization [4,18–22] (modulo an integer)

$$P = \frac{1}{2\pi} \int_0^{2\pi} dk A(k), \quad A(k) = i \sum_{\alpha \in \text{occ}} \langle u_\alpha(k) | \partial_k | u_\alpha(k) \rangle. \tag{5}$$

Note that P is quantized in units of $\frac{1}{2}$ in class AIII, since $\langle u_\alpha(k) | \partial_k | u_\alpha(k) \rangle = \langle S u_\alpha(k) | \partial_k | S u_\alpha(k) \rangle$; hence, the polarizations of the negative and positive energy bands are equal and their sum must be an integer. The connection between ν and P is particularly useful when disorder is present because P can be efficiently computed from the Wannier centers of the occupied states, providing an alternative numerical method to explore ν in the presence of disorder, although only modulo 2 (see the Supplemental Material [15]).

We now derive a covariant real-space representation of ν in any odd space dimensions, which remains well defined in the presence of disorder and can be evaluated with extreme precision using the methods elaborated in Refs. [5,28–31]. It is more convenient to work with the homotopically equivalent flatband Hamiltonian: $Q = P_+ - P_-$, where $P_\pm$ are the projectors onto the positive or negative energy spectrum. Since $S^\dagger = S$ and $S^2 = 1$, its eigenvalues are ± 1; hence, $S = S_+ - S_-$, with $S_\pm$ being the corresponding spectral projectors. Any chiral-symmetric operator, in particular, Q, decomposes as $Q = S_+ Q S_- + S_- Q S_+$, and the following relations are always true: $(S_\pm Q S_\mp)^\dagger = S_\mp Q S_\pm = (S_\pm Q S_\mp)^{-1}$ (viewed as maps between $S_\pm \mathcal{H}$, where $\mathcal{H}$ is the Hilbert space of the system). These provide the covariant, real-space form of the off-diagonal term (and its inverse) entering the winding number formula $Q_{+-} = S_+ Q S_-$, $(Q_{+-})^{-1} = S_- Q S_+ = Q_{-+}$. By recalling that $\int_0^{2\pi} (dk/2\pi) \times \text{tr}\{\}$ and ∂_k can be represented in real space as a trace per volume (denoted here by $\mathcal{T}\{\}$) and as the commutator $-i[X,]$ ($X =$ the position operator), respectively, the k-space expression [2] of ν in $2n + 1$ dimensions becomes

$$\nu = \frac{-(\pi i)^n}{(2n+1)!!} \sum_\rho (-1)^\rho \mathcal{T} \left\{ \prod_{i=1}^{2n+1} Q_{-+} [X_{\rho_i}, Q_{+-}] \right\}, \tag{6}$$

where the summation is over all possible permutations ρ of the indices. In 1D, $\nu = -\mathcal{T}\{Q_{-+}[X, Q_{+-}]\}$, which is the formula used in the present work. These real-space formulas can be evaluated in the presence of disorder, and it is important to note that they are self-averaging, so the result of a computation is independent of the disorder configuration being used.

Let us fix $m = 0.5$, in which case $\nu = 1$ at $W_{1,2} = 0$. In the limit $W_2 \to \infty$, the on-site potential becomes dominant and it commutes with X; hence, $\nu = 0$ in this limit. As such, a topological phase transition takes place, which we explored with Eq. (6). The behavior of ν with increasing disorder is reported in Fig. 1, where one can see ν staying quantized and nonfluctuating even after the spectral gap closes from the strong disorder (no disorder averaging is necessary). Upon further increase of disorder, an abrupt switch occurs from the topological $\nu = 1$ to the trivial $\nu = 0$ value, accompanied by strong fluctuations during the transition period. This behavior leaves little doubt that a topological critical point is lurking underneath. In fact, the analytic formula for the localization length, which is developed next, shows that the topological transition is accompanied by an Anderson localization-delocalization transition.

Because of a simplification occurring at $E = 0$, the localization length of the disordered model and the critical exponents at the critical point can be computed exactly at the Fermi level ($E = 0$). Indeed, the Schrödinger equation $H\psi = 0$ reads $t_n \psi_{n-\alpha,\alpha} + i\alpha m_n \psi_{n,\alpha} = 0$, where $\alpha = \pm 1$ represents the A and B sites, respectively. The solution is

$$\psi_{n+\xi_\alpha,\alpha} = i^n \prod_{j=1}^{n} \left(\frac{t_j}{m_j} \right)^\alpha \psi_{\xi_\alpha,\alpha},$$

where $\xi_\alpha = 0, 1$ for $\alpha = \pm 1$, respectively, leading to

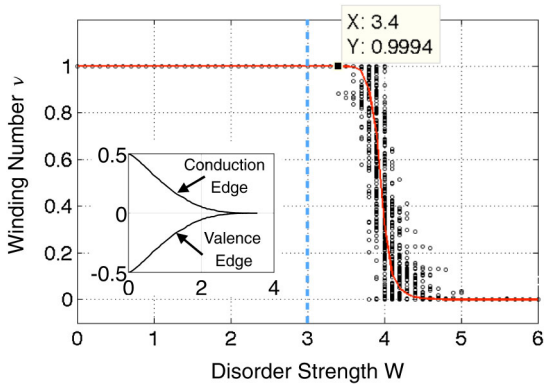

FIG. 1 (color online). Evolution of the winding number ν [Eq. (6)] with disorder: $W_1 = 0.5W$ and $W_2 = W$. The raw, unaveraged data for 200 disorder configurations are shown by the scattered points and the average by the solid line. Inset: The conduction and valence edges as functions of W, indicating a spectral gap closing at $W \approx 3$ (marked by the dashed line in the main panel). The marked data point reports a quantized $\nu = 0.9994$, at disorder well beyond $W = 3$.

$$\Lambda^{-1} = \max_{\alpha=\pm 1}\left[-\lim_{n\to\infty}\tfrac{1}{n}\log|\psi_{n+\xi_\alpha,\alpha}|\right] = \left|\lim_{n\to\infty}\tfrac{1}{n}\textstyle\sum_{j=1}^{n}(\ln|t_j| - \ln|m_j|)\right|.$$

According to Birkhoff's ergodic theorem, we can use the ensemble average to evaluate the last expression:

$$\Lambda^{-1} = \left|\int_{-1/2}^{1/2} d\omega \int_{-1/2}^{1/2} d\omega' (\ln|1 + W_1\omega| - \ln|m + W_2\omega'|)\right|.$$

The integrations can be performed explicitly, and in the regime of large W's where the arguments of the logarithms can become negative, we obtain

$$\Lambda^{-1} = \left|\ln\left[\frac{|2 + W_1|^{1/W_1+1/2}}{|2 - W_1|^{1/W_1-1/2}}\frac{|2m - W_2|^{m/W_2-1/2}}{|2m + W_2|^{m/W_2+1/2}}\right]\right|. \quad (7)$$

Using a numerical transfer matrix and level-spacing statistics analysis, we combed the energy spectrum and found that, in every instance, all the states at $E \neq 0$ are localized. Hence, for the critical behavior, we can focus exclusively on the case $E = 0$. This enables us to use Eq. (7) to draw the exact phase diagram in the three-dimensional parameter space (m, W_1, W_2) by tracing the critical surface $\mathcal{S}_c$ where $\Lambda \to \infty$. The result is shown in Fig. 2(a), which reveals that we are indeed dealing with two phases that are completely disconnected from each other. We can show that the phase inside $\mathcal{S}_c$ is a topological phase with $\nu = 1$, while outside $\mathcal{S}_c$, $\nu = 0$. As examples, in Figs. 2(b) and 2(c), we show calculations of ν from Eq. (6) for the sections defined by $W_2/W_1 = 2$ and $m = 0.5$, respectively, which confirms that the topological phase $\nu = 1$ extends all the way to the critical line, beyond which ν shifts abruptly to 0. By using the transfer matrix method [32], the localization length was also obtained

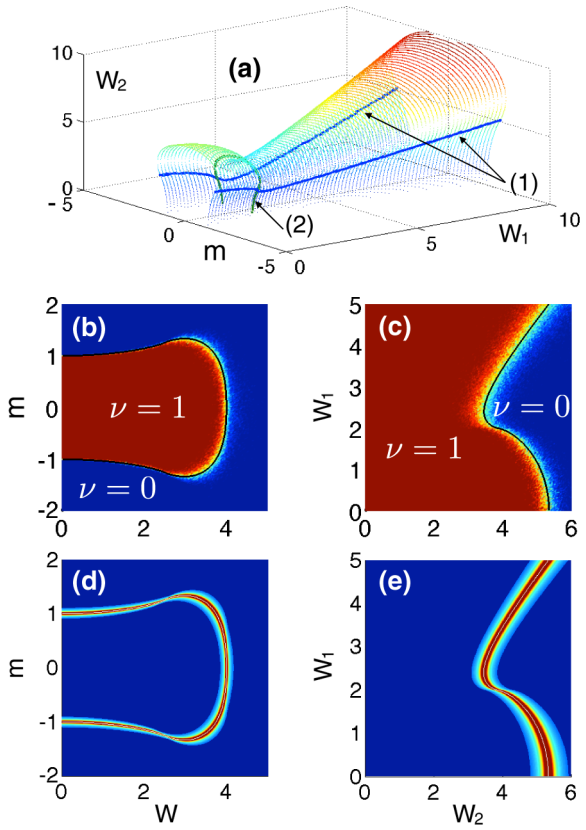

FIG. 2 (color online). (a) The critical surface ($\Lambda \to \infty$) in the three-dimensional phase space (m, W_1, W_2). The lines (1) and (2) represent the singular points where the scaling is anomalous (see the text). The next panels report maps of the (b),(c) winding number and (d),(e) localization length as computed with Eq. (6) and with the numerical transfer matrix method, respectively, for two sections of the phase space defined by the constraints (b), (d) $W_2 = 2W_1 = W$ and (c),(e) $m = 0.5$. The analytic critical curves are shown as black and white lines in (b),(c) and (d),(e), respectively. The computations of ν were done for $N = 1000$ and averaged over ten disorder configurations. The transfer matrix was iterated 10^8 times.

numerically in Figs. 2(d) and 2(e), where one can see a diverging critical line that matches perfectly with the analytic critical line from Eq. (7). Equation (7) also enables us to determine the critical exponent for the transition. Let (m_c, W_1^c, W_2^c) be a point on $\mathcal{S}_c$. We can cross $\mathcal{S}_c$ by varying any of the three parameters, so let us vary m in a small interval $[m_c - \epsilon, m_c + \epsilon]$. As shown in the Supplemental Material [15], $\Lambda^{-1}(m) = |m - m_c|[c_0 + c_1(m - m_c)^2 \ldots]$, which gives a critical exponent 1, except along lines (1) and (2) shown in Fig. 2(a), where the scaling has a logarithmic correction $\Lambda^{-1}(m) \sim |m - m_c| \ln|m - m_c|$.

We will now discuss the physical origin of the topological phase transition. Note that in 1D, there is no obstruction to defining exponentially localized Wannier functions in an insulating phase even if it is topological [23–27]. In fact, in the flatband limit ($m = 0$), we can find ultralocalized Wannier functions near each site n: $W_n^{(-)} = 1/\sqrt{2}(|n, B\rangle + |n + 1, A\rangle)$, having weight only on two

neighboring sites. When the system is tuned away from $m = 0$, but still in the topological phase, the Wannier functions will gradually spread but still remain exponentially localized at the midbond between sites n and $n+1$. Thus, this system and, in fact, all 1D topological insulator or superconductor phases can support a nontrivial integer topological invariant, even though the occupied states can be represented entirely using localized states. Additionally, the well-known levitation-annihilation process in free-fermion topological phases cannot possibly apply here because there are no delocalized bulk modes which carry the topological invariant. Instead, we will now show that each single-particle electron state carries part of the topological invariant, and because of this, a different type of disorder-driven transition must occur.

To proceed, we map Eq. (1) to a spin-1/2 Hamiltonian defined on a lattice of size $2N$ via the Jordan-Wigner transformation $c_{n,A} = (-i)^{n+1} K(2n) S^-_{2n}$ and $c_{n,B} = (-i)^n K(2n-1) S^-_{2n-1}$, where S^a_i are spin-1/2 variables and $K(m) = \exp(i\pi \sum_{j=1}^{m-1} S^+_j S^-_j)$ is the kink operator. These transformations lead to a Hamiltonian

$$H = \sum_i 2t_i (\hat{S}^x_{2i}\hat{S}^x_{2i+1} + \hat{S}^y_{2i}\hat{S}^y_{2i+1}) + 2m_i (\hat{S}^x_{2i}\hat{S}^x_{2i-1} + \hat{S}^y_{2i}\hat{S}^y_{2i-1}),$$

which is the spin-1/2 XX model with random exchange couplings $2t_i$ ($2m_{i+1}$) between the even (odd) bonds. There is a simple form of the ground state in the spin representation that simplifies the real-space description of the model. The ground state can be constructed by a real-space renormalization-group (RG) procedure which is asymptotically exact [33,34]. Each RG step consists of decimating the pair of spins that have the strongest exchange interaction by enforcing a spin-singlet state for that pair and correspondingly generating a new and weaker bond between the neighboring spins. The final result is the ground state in which each spin forms a singlet state with another spin in the system. For the generic case in which the distributions t_i and m_i are chosen to be different, the system is gapped and said to be dimerized [35]. Roughly speaking, the topological and trivial fermion phases correspond to dimerization patterns on either the odd or even bonds in the spin system, and these patterns are preserved during each RG step.

By the nature of the RG procedure, the singlets that are generated never cross each other, which implies that every singlet state in the ground state will be formed by one spin belonging to sublattice A and another spin belonging to sublattice B (a manifestation of the underlying chiral symmetry). Let us associate with the ith singlet a pair of numbers $d_i = \{d_{i1}, d_{i2}\}$ which are the lattice sites of the two spins in the singlet. The ground state is

$$|\Omega\rangle = \prod_i 1/\sqrt{2}[S^\dagger_{2d_{i1}} - S^\dagger_{2d_{i2}-1}]|\downarrow \ldots \downarrow\rangle. \quad (8)$$

If we map back to the fermion representation, the ground state can be simplified to $|\Omega\rangle = \prod_i 1/\sqrt{2}[\alpha_i c^\dagger_{d_{i1},A} - \beta_i c^\dagger_{d_{i2},B}]|0\rangle$, where α_i and β_i have unit modulus and depend on the configuration of the singlets (see the Supplemental Material [15]). This form of the ground state is remarkable because it is a product state constructed from the single-particle states $|\Phi_i\rangle = 1/\sqrt{2}(\alpha_i c^\dagger_{d_{i1},A} - \beta_i c^\dagger_{d_{i2},B})|0\rangle$ which, like the flatband limit in the disorder-free system, only have weight on two sites (although now the sites can be far apart). In this basis, the real-space winding number formula drastically simplifies to

$$\nu = \frac{1}{N}\sum_{i=1}^{N}(d_{i2} - d_{i1}), \quad (9)$$

which is just the sum of vectors connecting the end points of the singlets. In the clean topological phase, $(d_{i2} - d_{i1}) = 1$ and $\nu = 1/N \sum_i^N 1 = 1$, as expected. By contrast, in the trivial phase, singlets form on site, which implies $\nu = 1/N \sum_i^N 0 = 0$. This clearly illustrates that it is not a single delocalized state which carries the topological winding number but instead the entire set of occupied states. We could adiabatically deform the Hamiltonian while preserving chiral symmetry, so that states of the form $|\Phi_i\rangle$ become the single-particle eigenstates and then each state would carry a portion $1/N(d_{i2} - d_{i1})$ of ν.

We can further exploit the mapping to the spin model to understand the nature of the topological phase transition. Consider disordering a state that is dimerized on the even bonds (i.e., the topological state). From the RG procedure, one can see that disorder will favor the formation of regions that dimerize on the odd bonds, so that trivial and topological regions coexist. In the vicinity of the critical point, the low-energy interface states formed between these regions contribute to the spectral density inside the energy gap. This type of behavior corresponds to a Griffiths phase [35,36], which is not critical and thus explains why the topological invariant does not change at the gap closing point. The system becomes critical when dimerization occurs equally on both the odd and even bonds, leading to a proliferation of zero-energy interface states. As a result, both the localization length as well as the density of states become divergent at zero energy [37]. Similar physics, albeit in a different context involving superconducting wires, was discussed in Refs. [36,38], both of which are important precursors for our work. The critical point realizes the random singlet phase in which singlets are formed on all length scales [39]. The divergent length scale of singlet formation would appear to destabilize the winding number form in Eq. (9), as expected at criticality. To further support the claim that the topological phase transition is in the same universality class as the random singlet phase, we numerically confirmed (see the Supplemental Material [15]) that the critical scaling of the entanglement entropy contains the log 2 correction factor to the central charge, as expected [40]. Increasing the disorder beyond the critical point dimerizes the system on the odd bonds, which thus leads to the trivial state.

Coming back to the difference between the A and the AIII classes, we note that in class A, E_F can be positioned

anywhere in the energy spectrum and, when moving E_F to the global edges of the energy spectrum, a topological insulator will necessarily transition to a trivial phase somewhere along the way (since having all states occupied or all unoccupied is a trivial insulator), and consequently, bulk extended states will occur at the transition. This is why extended states exist in the energy spectrum of topological insulators from class A. This rationale, however, cannot be applied to class AIII because, here, E_F is fixed at $E = 0$. If E_F is shifted, then the matrix Q_{+-} is no longer unitary, so it can fail to be invertible and the winding number is no longer stable. As such, there is no reason for the existence of extended states above and below E_F in topological insulators from the AIII class.

In conclusion, we have given a complete picture of the physics of the disordered AIII class in 1D. We have given a real-space formula for the AIII winding number in all odd dimensions, shown that topological invariants can be carried by localized states, and shown that, because of this, the levitation and annihilation topological phase transition is replaced by the random singlet transition for the AIII class in 1D. It will be exciting to see if these types of effects can be seen in higher dimensions.

I. M.-S. and T. L. H. are supported by ONR Grant No. N0014-12-1-0935 and thank the UIUC ICMT for support. E. P. and J. S. acknowledge support by the U.S. NSF Grants No. DMS-1066045 and No. DMR-1056168. J. S. acknowledges additional support from the NSFC under Grant No. 11204065 and RFDPHE-China under Grant No. 20101303120005.

Note added.—Recently, another work on the AIII [and BDI (models in the Altland-Zirnbauer classification respecting particle-hole and time-reversal symmetry)] class appeared discussing the properties of disordered wires from a complementary renormalization-group point of view [41], with a focus on the quantum criticality near the topological transitions. There is some overlap between the discussions in the two articles, and where this happens, the conclusions agree. We believe that, together, these two works provide a well-rounded description of the disordered topological wires from the AIII class.

[1] A. P. Schnyder, S. Ryu, A. Furusaki, and A. W. W. Ludwig, Phys. Rev. B **78**, 195125 (2008).
[2] S. Ryu, A. P. Schnyder, A. Furusaki, and A. W. W. Ludwig, New J. Phys. **12**, 065010 (2010).
[3] A. Kitaev, AIP Conf. Proc. **1134**, 22 (2009).
[4] X.-L. Qi, T. L. Hughes, and S.-C. Zhang, Phys. Rev. B **78**, 195424 (2008).
[5] E. Prodan, T. L. Hughes, and B. A. Bernevig, Phys. Rev. Lett. **105**, 115501 (2010).
[6] E. Prodan, B. Leung, and J. Bellissard, J. Phys. A **46**, 485202 (2013).
[7] B. I. Halperin, Phys. Rev. B **25**, 2185 (1982).
[8] J. Bellissard, A. van Elst, and H. Schulz-Baldes, J. Math. Phys. (N.Y.) **35**, 5373 (1994).
[9] M. Onoda, Y. Avishai, and N. Nagaosa, Phys. Rev. Lett. **98**, 076802 (2007).
[10] Z. Xu, L. Sheng, D. Y. Xing, E. Prodan, and D. N. Sheng, Phys. Rev. B **85**, 075115 (2012).
[11] M. J. Gilbert, B. A. Bernevig, and T. L. Hughes, Phys. Rev. B **86**, 041401 (2012).
[12] B. Leung and E. Prodan, Phys. Rev. B **85**, 205136 (2012).
[13] P. Hosur, S. Ryu, and A. Vishwanath, Phys. Rev. B **81**, 045120 (2010).
[14] A. P. Schnyder, S. Ryu, and A. W. W. Ludwig, Phys. Rev. Lett. **102**, 196804 (2009).
[15] See Supplemental Material at http://link.aps.org/supplemental/10.1103/PhysRevLett.113.046802 for the proof of the relation between winding and polarization, the derivation of the decomposition of any chiral-symmetric operator, the derivation of the critical scaling, the proof of Eq. (9), and the numerical check of the scaling of the entanglement at the critical point and which includes Refs. [16,17].
[16] P. Calabrese and J. Cardy, J. Stat. Mech. (2004) P06002.
[17] G. Refael and J. E. Moore, J. Phys. A **42**, 504010 (2009).
[18] R. D. King-Smith and D. Vanderbilt, Phys. Rev. B **47**, 1651 (1993).
[19] G. Ortiz and R. M. Martin, Phys. Rev. B **49**, 14202 (1994).
[20] J. Zak, Phys. Rev. Lett. **62**, 2747 (1989).
[21] T. L. Hughes, E. Prodan, and B. A. Bernevig, Phys. Rev. B **83**, 245132 (2011).
[22] A. M. Turner, Y. Zhang, R. S. K. Mong, and A. Vishwanath, Phys. Rev. B **85**, 165120 (2012).
[23] S. Kivelson, Phys. Rev. B **26**, 4269 (1982).
[24] N. Marzari and D. Vanderbilt, Phys. Rev. B **56**, 12847 (1997).
[25] T. Thonhauser and D. Vanderbilt, Phys. Rev. B **74**, 235111 (2006).
[26] C. Brouder, G. Panati, M. Calandra, C. Mourougane, and N. Marzari, Phys. Rev. Lett. **98**, 046402 (2007).
[27] M. B. Hastings and T. A. Loring, J. Math. Phys. (N.Y.) **51**, 015214 (2010).
[28] T. A. Loring and M. B. Hastings, Europhys. Lett. **92**, 67004 (2010).
[29] E. Prodan, J. Phys. A **44**, 113001 (2011).
[30] M. B. Hastings and T. A. Loring, Ann. Phys. (Amsterdam) **326**, 1699 (2011).
[31] E. Prodan, Appl. Math. Res. **2013**, 176 (2013).
[32] A. MacKinnon and B. Kramer, Z. Phys. B **53**, 1 (1983).
[33] D. S. Fisher, Phys. Rev. B **50**, 3799 (1994).
[34] C. Dasgupta and S.-k. Ma, Phys. Rev. B **22**, 1305 (1980).
[35] R. A. Hyman, K. Yang, R. N. Bhatt, and S. M. Girvin, Phys. Rev. Lett. **76**, 839 (1996).
[36] O. Motrunich, K. Damle, and D. A. Huse, Phys. Rev. B **63**, 224204 (2001).
[37] L. Balents and M. P. A. Fisher, Phys. Rev. B **56**, 12970 (1997).
[38] I. A. Gruzberg, N. Read, and S. Vishveshwara, Phys. Rev. B **71**, 245124 (2005).
[39] D. S. Fisher, Phys. Rev. B **51**, 6411 (1995).
[40] G. Refael and J. E. Moore, Phys. Rev. Lett. **93**, 260602 (2004).
[41] A. Altland, D. Bagrets, L. Fritz, A. Kamenev, and H. Schmiedt, Phys. Rev. Lett. **112**, 206602 (2014).